

ORIGINAL RESEARCH

Open Access

A hybrid ENO reconstruction with limiters for systems of hyperbolic conservation laws

Arshad Ahmud Iqbal Peer^{1*}, Désiré Yannick Tangman² and Muddun Bhuruth²

Abstract

We consider a new class of essentially non-oscillatory (ENO) piecewise polynomial reconstructions together with interpolants based on Monotone Upwind Schemes for Conservation Laws. We improve the second-order ENO polynomial reconstruction by choosing an additional point inside the stencil in order to obtain the highest accuracy when combined with various non-linear limiters. The resulting algorithms are based on only one stencil selection, and we show that they can be efficiently implemented with largest allowable CFL numbers using optimal strong stability-preserving Runge-Kutta time evolution methods. The numerical results indicate that in some cases the schemes yield errors smaller in magnitude as compared to the fourth-order ENO scheme.

Keywords: Essentially non-oscillatory, Hyperbolic conservation laws, MUSCL-type interpolants, Nonlinear limiters

Introduction

In this paper, we review and modify the essentially non-oscillatory (ENO) reconstruction of [1] for the approximate solution of hyperbolic conservation laws

$$u_t + f(u)_x = 0, \quad u \in \mathbb{R}^d, \quad d \geq 1, \quad (1)$$

with initial data $u(x, 0) = u_0(x)$.

For the sake of simplicity, we first consider scalar conservation laws, that is, $d = 1$ in (1). The discretisation of (1) is done on a uniform spatial grid where the cell $I_j = [x_{j-1/2}, x_{j+1/2}]$ has a width h . Also, let $x_j = \frac{1}{2}(x_{j-1/2} + x_{j+1/2})$ be the mid-cell grid point of I_j . Integrating (1) over the cell I_j leads to the semi-discrete conservation equation that samples solutions at cell centres and can be formulated as

$$\frac{d\bar{u}_j(t)}{dt} = -\frac{1}{h} \left[\hat{f}_{j+\frac{1}{2}} - \hat{f}_{j-\frac{1}{2}} \right], \quad (2)$$

where the cell average of u on I_j is given by $\bar{u}_j \equiv \frac{1}{h} \int_{I_j} u(x, t) dx$ and the exact flux is $\hat{f}_{j+\frac{1}{2}} \equiv f(u(x_{j+\frac{1}{2}}, t))$.

The computation of the flux at cell boundaries requires a polynomial reconstruction that has been the subject of considerable work [1-4].

ENO reconstructions aim to achieve high accuracy in smooth regions in addition to resolving discontinuities with correct positions by adaptively selecting the smoothest stencil among several candidates without introducing spurious oscillations. The authors in [5,6] showed that the weighted ENO (WENO) schemes [3,4,7], both upwind or central based, fail to satisfy the sign property. Furthermore, they showed that ENO reconstructions and interpolation procedures are stable.

However, low-order ENO schemes have been observed to smear discontinuities [8] and smoothing up of corners [9]. Higher-order ENO reconstructions decrease damping but generate significant oscillations when solving hyperbolic systems unless costly characteristic decompositions are used [10]. Also, Xu and Shu [11] noted that it is not possible to maintain the non-oscillatory property and at the same time avoid the smearing of discontinuities by high-order ENO schemes.

The works of [12-14] demonstrated that hybridized schemes perform better than the existing schemes by taking advantages of each of their components. For example, the authors in [15-17] proposed the use of limiters in conjunction with ENO reconstructions. The numerical experiments described in those works show that the modified scheme reduced smearing near discontinuities and gave good resolutions of corners and local extremas. Furthermore, different ENO-type methods have been extended to multi-dimensional problems, see for example

*Correspondence: apeer@umail.utm.ac.mu

¹Department of Applied Mathematical Sciences, University of Technology, Mauritius, La Tour Koenig, Pointe-aux-Sables, Mauritius
Full list of author information is available at the end of the article

[15,18-21], and Serna and Marquina [15] noted that some ENO methods combined with limiters performed better than conventional ENO methods of similar order for multi-dimensional problems where fine structures appear to be important.

This paper proposes a new hybrid scheme that reduces the damping near discontinuities. Our technique avoids the costly characteristic decomposition and is based on modifying the second-order ENO polynomial reconstruction to obtain a higher-order polynomial combined with non-linear limiters to avoid spurious oscillations. Instead of using a reconstruction over two cells for finding the fluxes of (2), we use an additional point within the stencil by means of a MUSCL-type interpolant [22] with numerical derivatives. Those derivatives depend on non-linear limiters that vary according to the smoothness of its vicinity and improve the behaviour of the scheme near discontinuities.

We give an outline of this paper. We first describe the new reconstructions with various interpolants and limiters. We then give the results of numerical experiments for our schemes, and we extend the new class of hybrid schemes to solve hyperbolic systems of conservation laws. The conclusions on this work are presented in the final section.

Methods

A hybrid ENO-flux limiter scheme

We use a finite volume approach for one-dimensional equations, and we approximate $u(x_j, t)$ by u_j . Assuming that the cell averages \bar{u}_j are known at time t , Harten et al. [1] proposed a piecewise polynomial reconstruction $u(x, t) = \sum_j p_j(x) \chi_j(x)$ to solve (2), where $\chi_j(x)$ is the characteristic function of the cell I_j . In the second-order ENO2 reconstruction, $p_j(x)$ is a linear polynomial on the cell I_j , and it maintains conservation, that is, $\frac{1}{h} \int_{I_j} p_j(x) dx = \bar{u}_j$.

The two-cell stencils of ENO2 are obtained by either choosing $r = 0$ or $r = 1$ cell to the right of I_j . Let $V(x)$ be the primitive function of $u(x, t)$, that is, $V(x) = \int_{-\infty}^x u(\xi, t) d\xi$. Then interpolating $V(x)$ at the cell boundaries $x_{j-r+i-1/2}$ for $i = 0, 1, 2$ by using Newton's interpolation formula and differentiating the new polynomial, we get

$$p_j(x) = \sum_{i=1}^2 V \left[x_{j-r-\frac{1}{2}}, \dots, x_{j-r+i-\frac{1}{2}} \right] \times \sum_{m=0}^{i-1} \prod_{l=0, l \neq m}^{i-1} (x - x_{j-r+l-\frac{1}{2}}), \quad (3)$$

where V is a divided difference. The 0th-degree divided difference of $V(x)$ is simply $V[x_{j+1/2}] \equiv V(x_{j+1/2})$. The ENO polynomials approximate the cell boundaries of (2)

by taking $u_{j+1/2}^- = p_j(x_{j+1/2})$ and $u_{j+1/2}^+ = p_{j+1}(x_{j+1/2})$. An evolution step consists of collecting the point values $u(x_{j+1/2}, t)$ from $u_{j+1/2}^-$ and $u_{j+1/2}^+$, and $\hat{f}_{j+\frac{1}{2}} = h(u_{j+\frac{1}{2}}^-, u_{j+\frac{1}{2}}^+)$, where $h(\cdot, \cdot)$ is a monotone flux. Some possible choices for these class of schemes are the Godunov, Lax-Friedrichs and Roe with entropy fix fluxes. The advantages and disadvantages associated with these fluxes are discussed by [8]. In this paper, we will use the Lax-Friedrichs flux.

We start the new reconstruction by selecting a two-cell stencil as for the ENO scheme. Let $y_i = x_{j+i-r-1/2}$ for $i = 0, 1$ and 2 denote the cell boundaries of the stencil. The next step consists of adding another point $y_3 = x_j \in I_j$. The interpolating polynomial is then given by

$$p_j(x) = \sum_{i=1}^3 V[y_0, \dots, y_i] \sum_{m=0}^{i-1} \prod_{l=0, l \neq m}^{i-1} (x - y_l). \quad (4)$$

In order to compute the divided differences of (4), we need a polynomial that retains information within the cells I_j . Nessyahu and Tadmor [23] used a second-order MUSCL interpolant

$$L_j(x) = \bar{u}_j + (x - x_j) \frac{1}{h} u'_j, \quad x \in I_j, \quad (5)$$

to compensate for the numerical viscosity introduced by the Lax-Friedrichs scheme [24]. Since $\frac{1}{h} \int_{I_j} L_j(x) dx = \bar{u}_j$, polynomial (5) retains conservation. The divided difference $V[y_2, y_3]$ given by

$$V[y_2, y_3] = \frac{1}{x_j - x_{j-r+3/2}} \times \left(\int_{-\infty}^{x_j} u(x) dx - \int_{-\infty}^{x_{j-r+3/2}} u(x) dx \right)$$

is computed using the MUSCL interpolant (5), such that $u(x) = \sum_j L_j(x) \chi_j(x)$, where $\chi_j(x)$ is the characteristic function of I_j . The divided differences are found to be

$$V[y_2, y_3] = \frac{(1 + 2r)(4\bar{u}_j + u'_j) + 8(1 - r)\bar{u}_{j+1}}{12}, \quad r = 0, 1. \quad (6)$$

From (4) and (6), we deduce the following approximations at the cell boundaries $x_{j+\frac{1}{2}}$:

If

$$\left| V \left[x_{j-\frac{3}{2}}, x_{j-\frac{1}{2}}, x_{j+\frac{1}{2}} \right] \right| \leq \left| V \left[x_{j-\frac{1}{2}}, x_{j+\frac{1}{2}}, x_{j+\frac{3}{2}} \right] \right|,$$

we take

$$u_{j+\frac{1}{2}}^{-(1)} = \frac{1}{6} (\bar{u}_{j-1} + 5\bar{u}_j + 4u'_j), \quad (7)$$

$$u_{j+\frac{1}{2}}^{+(1)} = \frac{1}{6} (\bar{u}_j + 5\bar{u}_{j+1} - 2u'_{j+1}); \quad (8)$$

otherwise

$$u_{j+\frac{1}{2}}^{-(0)} = \frac{1}{6}(5\bar{u}_j + \bar{u}_{j+1} + 2u'_j), \quad (9)$$

$$u_{j+\frac{1}{2}}^{+(0)} = \frac{1}{6}(5\bar{u}_{j+1} + \bar{u}_{j+2} - 4u'_{j+1}). \quad (10)$$

For the numerical derivative u'_j , we first consider the non-linear limiter of [23]:

$$u'_j = \text{MM} \left\{ \theta \Delta \bar{u}_{j+\frac{1}{2}}, \frac{1}{2}(\bar{u}_{j+1} - \bar{u}_{j-1}), \theta \Delta \bar{u}_{j-\frac{1}{2}} \right\}, \quad (11)$$

where the differences are given by $\Delta \bar{u}_{j+1/2} = \bar{u}_{j+1} - \bar{u}_j$ and $\Delta^2 \bar{u}_j = \bar{u}_{j+1} - 2\bar{u}_j + \bar{u}_{j-1}$. The MinMod limiter MM is set as

$$\text{MM}\{x_1, x_2, \dots\} = \begin{cases} \min_p \{x_p\} & \text{if } x_p > 0 \forall p, \\ \max_p \{x_p\} & \text{if } x_p < 0 \forall p, \\ 0 & \text{otherwise.} \end{cases}$$

The classical MinMod limiter with $\theta = 1$ (MM1) is second-order accurate and gives the numerical derivative

$$u'_j = \text{MM} \left\{ \Delta \bar{u}_{j+\frac{1}{2}}, \Delta \bar{u}_{j-\frac{1}{2}} \right\}, \quad (12)$$

which is non-oscillatory in the sense that

$$0 \leq u'_j \cdot \text{sign}(\Delta \bar{u}_{j\pm\frac{1}{2}}) \leq \text{Const.} \cdot \left| \text{MM} \left(\Delta \bar{u}_{j-\frac{1}{2}}, \Delta \bar{u}_{j+\frac{1}{2}} \right) \right|.$$

Since MM1 may oversmear some discontinuities [23], we can instead choose $\theta = 2$ (MM2) to have a steeper slope, unless oscillations are present, in which case we let $u'_j = 0$. This mechanism is aimed to reduce spurious oscillations allowed by other reconstructions like ENO [1] and WENO [3]. A Taylor expansion of the cell averages about the cell boundaries shows that the reconstructions (7), (8), (9) and (10) combined with the different values of the MinMod limiter vary from first-order near discontinuities up to third order in smooth regions.

In the numerical examples, we also combine the newly developed reconstructions with the following two non-linear limiters:

- (a) *UNO limiter*. The accuracy of (12) drops at the non-sonic critical grid values u_j , where $\Delta u_{j-\frac{1}{2}} \cdot \Delta u_{j+\frac{1}{2}} < 0 \neq f'(u_j)$ [25,26]. The UNO limiter [27] adds second-order differences to the MinMod limiter (12) to achieve high accuracy including at critical points

$$u'_j = \text{MM} \left\{ \Delta \bar{u}_{j-\frac{1}{2}} + \frac{1}{2} \text{MM} \left\{ \Delta^2 \bar{u}_{j-1}, \Delta^2 \bar{u}_j \right\}, \Delta \bar{u}_{j+\frac{1}{2}} - \frac{1}{2} \text{MM} \left\{ \Delta^2 \bar{u}_j, \Delta^2 \bar{u}_{j+1} \right\} \right\}. \quad (13)$$

This feature retains information about the slopes of the solution. However, it uses a wider stencil with respect to existing ENO reconstructions of

comparable accuracy. This stencil allows the limiter to avoid discontinuities, and in case extremas cannot be avoided, the accuracy of the UNO limiter decreases until a non-oscillatory approximation is obtained. Contrary to the power limiter of [15] which influences only second-order derivatives, the UNO limiter fully adapts the accuracy of our proposed polynomial reconstruction to the approximated profile. A Taylor expansion of the cell averages of the approximations (7) to (10) combined with the UNO limiter gives up to third-order accuracy.

- (b) *Harmod limiter* [15] is the harmonic mean of two differences of the same sign

$$u'_j = \left(\text{sign} \left(\Delta \bar{u}_{j-\frac{1}{2}} \right) + \text{sign} \left(\Delta \bar{u}_{j+\frac{1}{2}} \right) \right) \frac{\left| \Delta \bar{u}_{j-\frac{1}{2}} \right| \left| \Delta \bar{u}_{j+\frac{1}{2}} \right|}{\left| \Delta \bar{u}_{j-\frac{1}{2}} \right| + \left| \Delta \bar{u}_{j+\frac{1}{2}} \right|}.$$

Higher-order interpolant

A smoother limiter can be obtained for the proposed scheme by using a higher-order piecewise polynomial, which in turn can be obtained using the third-order non-oscillatory reconstruction due to [28]. This reconstruction seeks quadratic polynomials of the form:

$$q_j(x) = a_j + b_j \left(\frac{x - x_j}{h} \right) + c_j \left(\frac{x - x_j}{h} \right)^2,$$

such that the piecewise parabolic reconstruction satisfies the properties of conservation, $\frac{1}{h} \int_{I_j} q_j(x) dx = \bar{u}_j$. It is also third-order accurate, that is, $q_j(x) = u(x) + O(h^3)$. In addition, the quadratic polynomial interpolates the two neighbouring cell averages $\bar{u}_{j\pm 1}$. These three constraints uniquely determine the coefficients as $a_j = (\bar{u}_j - \frac{1}{24} \Delta^2 \bar{u}_j)$, $b_j = \Delta_0 \bar{u}_j$ and $c_j = \frac{1}{2} \Delta^2 \bar{u}_j$. Finally, in order to avoid spurious extremas at the cell interfaces, a convex modification of the form $L_j(x) = \bar{u}_j + \theta_j (q_j(x) - \bar{u}_j)$ and $0 < \theta_j < 1$ is used where the limiter θ_j is sought such that $(1 - \theta_j)$ is proportional to the interface jump $q_{j+1}(x_{j+\frac{1}{2}}) - q_j(x_{j+\frac{1}{2}})$.

The limiter θ_j is constructed in terms of the following cell quantities:

$$M_j = \max_{x \in I_j} q_j(x), \quad m_j = \min_{x \in I_j} q_j(x),$$

and

$$M_{j\pm\frac{1}{2}} = \max \left\{ \frac{1}{2}(\bar{u}_j + \bar{u}_{j\pm 1}), q_{j\pm 1}(x_{j\pm\frac{1}{2}}) \right\},$$

$$m_{j\pm\frac{1}{2}} = \min \left\{ \frac{1}{2}(\bar{u}_j + \bar{u}_{j\pm 1}), q_{j\pm 1}(x_{j\pm\frac{1}{2}}) \right\},$$

Table 1 L_1 errors and orders of convergence and CPU times for Problem 1

	MM1	MM2	UNO	Harmod	Quadratic	ENO3
N						
160	3.383(-2)	1.824(-3)	2.110(-4)	6.483(-3)	2.110(-4)	2.110(-4)
320	9.713(-3)	3.503(-4)	2.638(-5)	1.435(-3)	2.638(-5)	2.638(-5)
640	2.639(-3)	6.566(-5)	3.298(-6)	3.132(-4)	3.298(-6)	3.298(-6)
L_1 order	1.88	2.42	3.00	2.20	3.00	3.00
Time (s) for $N = 160$	0.8112	0.9449	1.0731	0.8290	5.1081	1.0109

and is given in [29] as

$$\theta_j = \begin{cases} \min \left\{ \frac{M_{j+\frac{1}{2}} - \bar{u}_j}{M_j - \bar{u}_j}, \frac{m_{j-\frac{1}{2}} - \bar{u}_j}{m_j - \bar{u}_j}, 1 \right\}, & \text{if } \bar{u}_{j-1} < \bar{u}_j < \bar{u}_{j+1}, \\ \min \left\{ \frac{M_{j-\frac{1}{2}} - \bar{u}_j}{M_j - \bar{u}_j}, \frac{m_{j+\frac{1}{2}} - \bar{u}_j}{m_j - \bar{u}_j}, 1 \right\}, & \text{if } \bar{u}_{j-1} > \bar{u}_j > \bar{u}_{j+1}, \\ 1, & \text{otherwise.} \end{cases} \quad (14)$$

The quadratic interpolant can then be written as follows:

$$L_j(x) = u_j + u'_j \left(\frac{x - x_j}{h} \right) + \frac{1}{2} u''_j \left(\frac{x - x_j}{h} \right)^2, \quad x \in I_j, \quad (15)$$

where $u'_j = \theta_j \Delta_0 \bar{u}_j$, $u''_j = \theta_j \Delta^2 \bar{u}_j$ and $u_j = \bar{u}_j - \frac{1}{24} u''_j$. Considering the additional point $y_3 = x_j \in I_j$ to compute the divided differences $V[y_2, y_3]$ and using (15), we get (6). Thus, as before, we get the approximations (7), (8), (9) and (10) at the cell boundaries, and where now the numerical derivatives dependent on (14). We recover third-order accurate ENO spatial reconstructions when the parameter $\theta_j = 1$ in smooth regions.

We remark that the hybrid reconstructions can be extended to ENO schemes of any order by interpolating

the primitive values at cell boundaries along with the additional point x_j . The first-order divided difference containing x_j of the interpolating polynomial is evaluated using a conservative piecewise polynomial with numerical derivatives of similar accuracy as the ENO scheme. Those numerical derivatives are chosen to be non-oscillatory in the sense of (W)ENO schemes [1,3] or to damp spurious oscillations as in [23,30].

Results and discussion

Scalar test problems

We describe the results of numerical experiments using some scalar test problems. The scalar test problems have periodic boundary conditions and are solved on the interval $[-1, 1]$. The p th-order ENO scheme is denoted by ENO p , and the hybrid schemes by the limiter used. The higher-order hybrid reconstruction with the quadratic polynomial (15) is denoted as Quadratic. All the reconstructions are combined with the Lax-Friedrichs flux [8] and with strong stability-preserving Runge-Kutta (SSPRK) methods [31-33]. The experiments are carried out in MATLAB environment on a 1.91-GHz processor with 992 MB of RAM.

Problem 1. We consider the linear advection equation $u_t + u_x = 0$ with the continuous initial condition $u(x, 0) =$

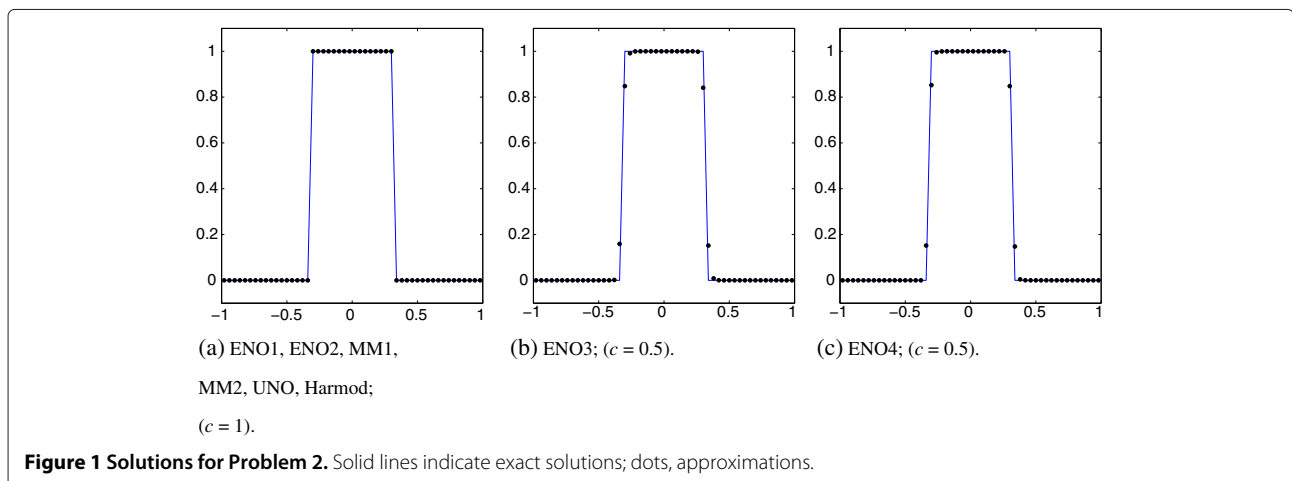


Table 2 L_1 errors and CPU times of solutions of Problem 3 for $T = 0.64$

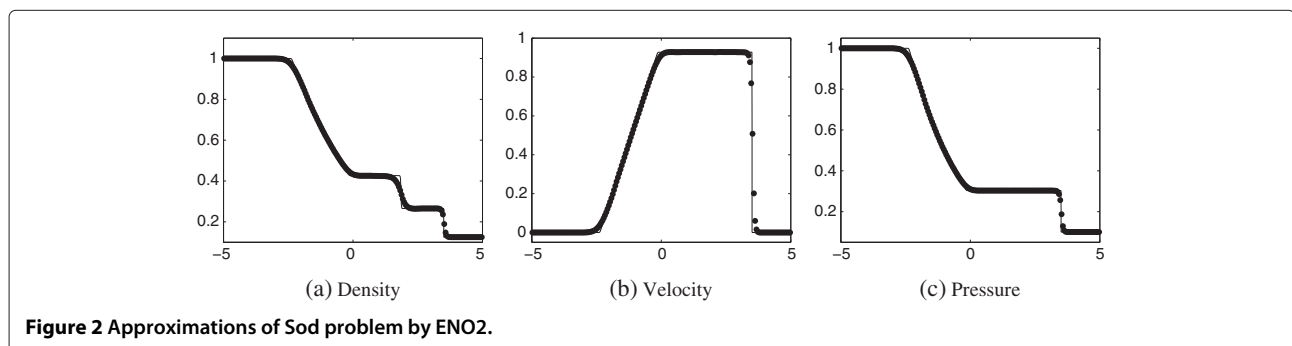
	Number of cells			
	40	80	160	320
ENO1				
L_1 error	1.617(-1)	9.632(-2)	5.657(-2)	3.293(-2)
Time (s)	0.0034	0.0072	0.0163	0.0410
ENO2				
L_1 error	6.951(-2)	3.325(-2)	1.903(-2)	1.087(-2)
Time (s)	0.0060	0.0121	0.0271	0.0704
ENO3				
L_1 error	5.327(-2)	2.488(-2)	1.521(-2)	8.926(-3)
Time (s)	0.0088	0.0179	0.0401	0.1049
ENO4				
L_1 error	4.758(-2)	2.081(-2)	1.404(-2)	9.943(-3)
Time (s)	0.0120	0.0242	0.0564	0.1500
MM1				
L_1 error	7.292(-2)	3.551(-2)	1.968(-2)	1.113(-2)
Time (s)	0.0067	0.0146	0.0334	0.0892
MM2				
L_1 error	5.205(-2)	2.487(-2)	1.503(-2)	8.728(-3)
Time (s)	0.0076	0.0164	0.0386	0.1035
UNO				
L_1 error	5.942(-2)	2.778(-2)	1.651(-2)	9.389(-3)
Time (s)	0.0088	0.0185	0.0430	0.1138
Harmod				
L_1 error	5.787(-2)	2.743(-2)	1.608(-2)	9.293(-3)
Time (s)	0.0067	0.0149	0.0345	0.0892
Quadratic				
L_1 error	5.484(-2)	2.893(-2)	1.518(-2)	-
Time (s)	0.1550	0.4436	1.3727	-

$\sin(\pi x)$. We solve the problem up to time $T = 10$ using the third-order SSPRK scheme with the CFL number $c = 0.45$. The results for the hybrid schemes are shown in Table 1. The L_1 order of convergence is for 320 to 640 cells used during the computations, and the CPU times

are for 160 cells. The hybrid schemes, which require a stencil selection only once, give better results than ENO1 and ENO2 as expected. The hybrid scheme with the limiter MM1 produces error of the same order as ENO2. The limiters MM2 and Harmod achieve rates of convergence greater than 2, whereas UNO and Quadratic produce third-order results as ENO3. However, the hybrid scheme with the quadratic piecewise polynomial (15) requires significantly more time to run. MM1, MM2 and Harmod limiters have comparable CPU times to ENO2, whereas UNO limiter gives CPU times of similar order to ENO3.

Problem 2. We consider the linear advection equation $u_t + u_x = 0$ with initial condition given by the square wave $u(x, 0) = 1$ for $|x| < 1/3$ and 0 elsewhere. Figure 1 shows the results obtained at time $T = 4$ using 50 equally spaced cells. We observe that the hybrid schemes approximate the exact solution with high accuracy for $c = 1$. ENO3 and ENO4 become unstable and diverge for $c = 1$. Figure 1b,c gives the ENO3 and ENO4 solutions for $c = 0.5$, where the solutions are damped near the discontinuities in both cases.

Problem 3. Our next experiment consists of the inviscid Burgers' equation $u_t + (0.5u^2)_x = 0$ with the discontinuous initial condition $u(x, 0) = 1$ for $|x| < 1/3$ and 0 elsewhere. In Table 2, we give the L_1 error and CPU time of the different solutions for $T = 0.64$. The time evolution process for the different schemes is done with the third-order SSPRK scheme and $c = 0.8$. We see that as expected, ENO1 produces the largest error. ENO2 and the hybrid scheme with the limiter MM1 produce numerical solutions of comparable accuracy. The remaining hybrid schemes give results of comparable accuracy to ENO3 and ENO4. The hybrid schemes with the MM1 and Harmod limiters have comparable CPU times to ENO2, whereas using the MM2 and UNO limiters give timings of the same order as ENO3. The Quadratic limiter is again the slowest of the different hybrid schemes and diverges on refined grids for large CFL numbers.



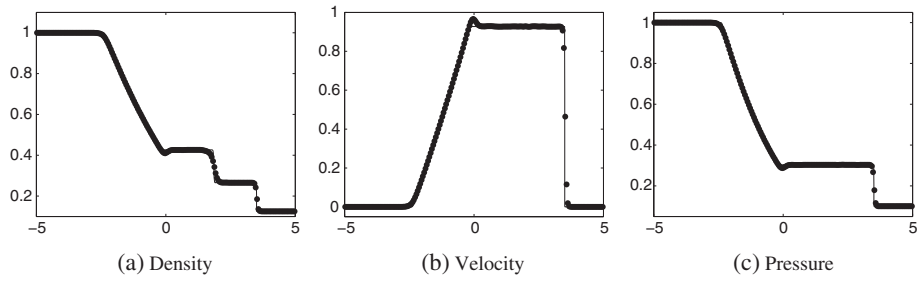


Figure 3 Approximations of Sod problem by ENO3.

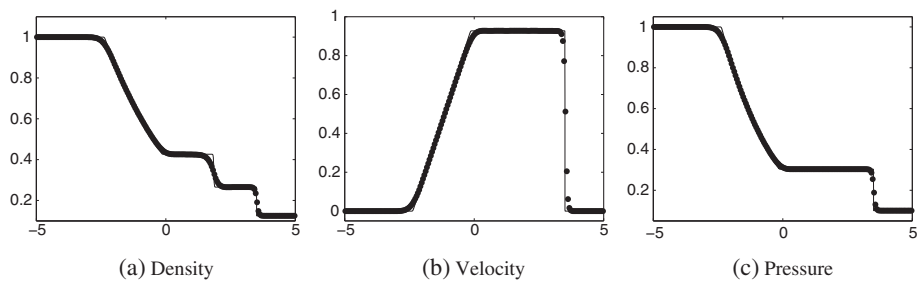


Figure 4 Approximations of Sod problem by MM1.

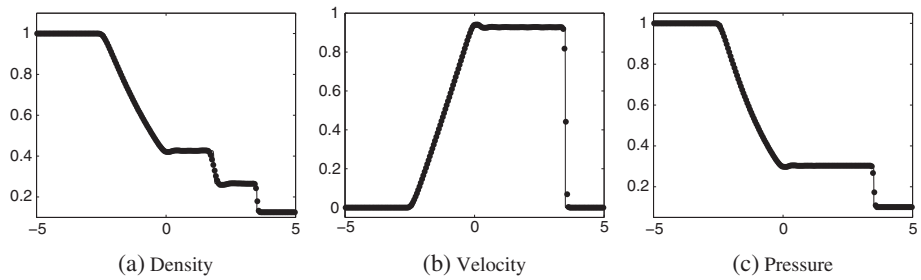


Figure 5 Approximations of Sod problem by MM2.

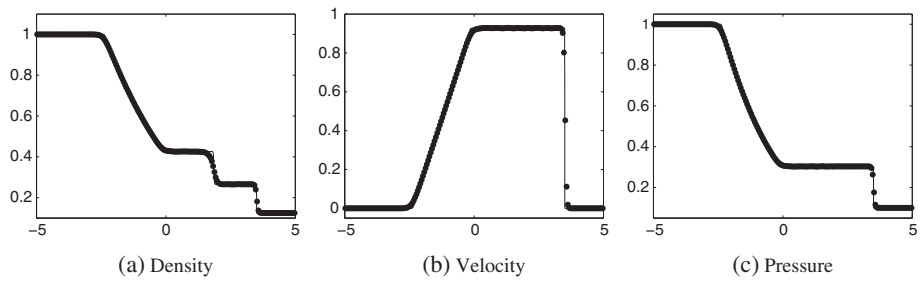
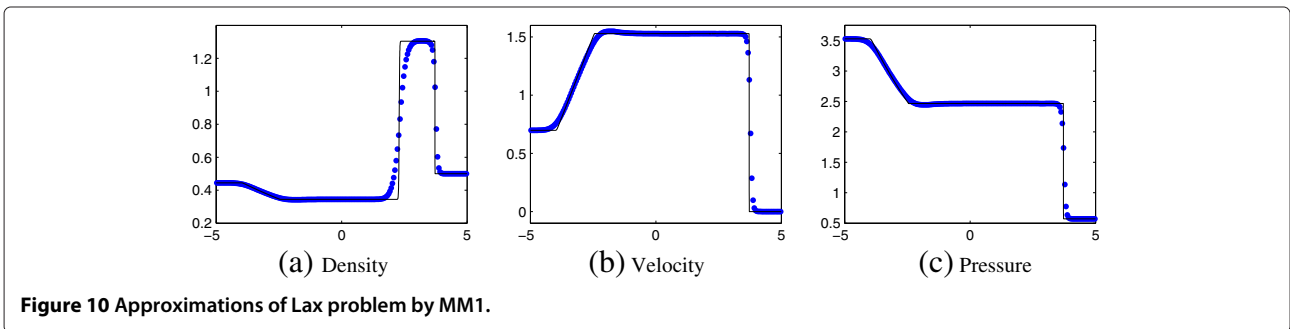
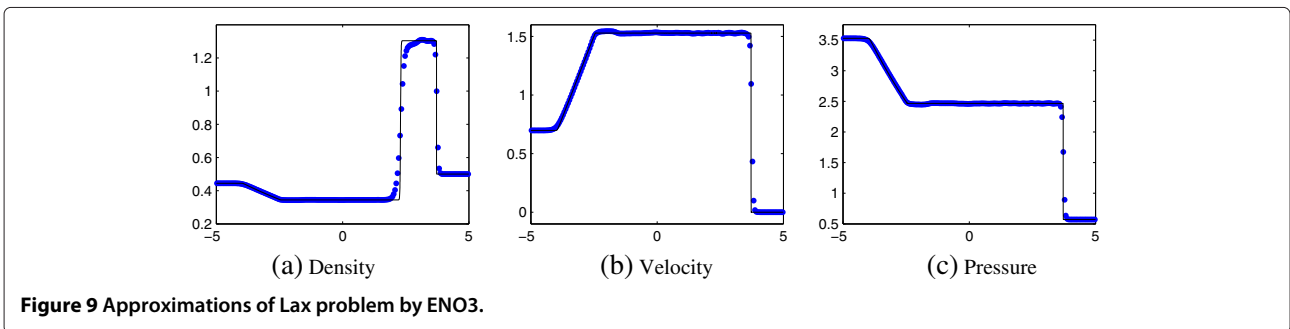
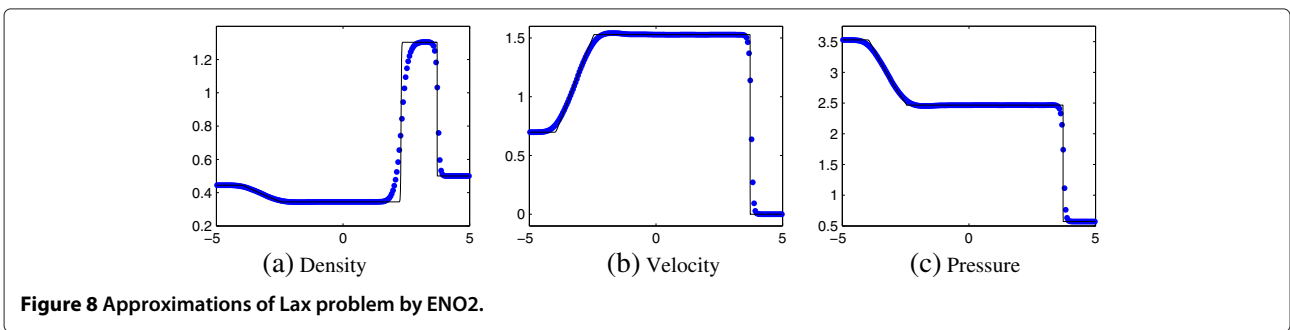
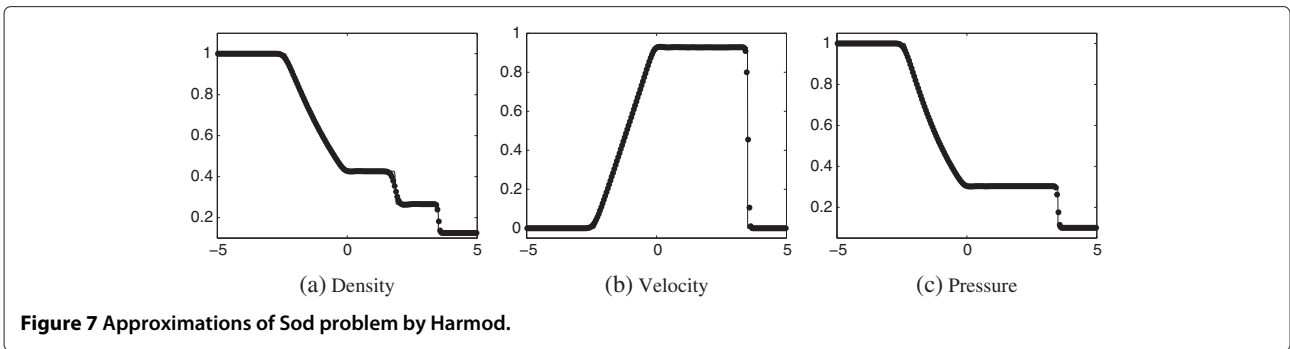
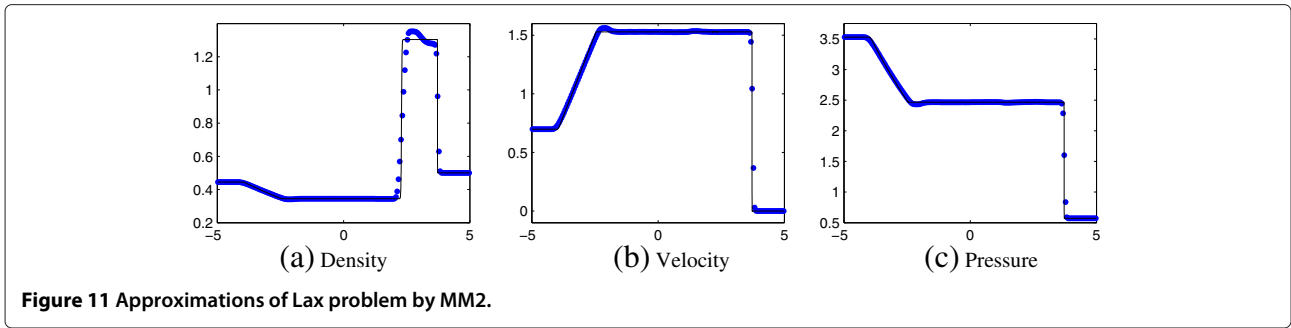


Figure 6 Approximations of Sod problem by UNO.





Systems of conservation laws

We extend our scheme to solve one-dimensional hyperbolic systems of conservation laws for (1) of the type

$$U_t + F(U)_x = 0. \tag{16}$$

The Jacobian $A(u)$ of the flux $F(u)$ has distinct real eigenvalues.

At present, we pay more attention to solve the Euler equations of gas dynamics for a polytropic gas:

$$\frac{\partial}{\partial t} \begin{bmatrix} \rho \\ \rho q \\ E \end{bmatrix} + \frac{\partial}{\partial x} \begin{bmatrix} \rho q \\ \rho q^2 + p \\ q(E + p) \end{bmatrix} = 0, \quad p = (\gamma - 1)(E - \frac{1}{2}\rho q^2). \tag{17}$$

Here ρ , q , p and E are respectively the density, velocity, pressure and total energy of the conserved fluid, and the ratio of the specific heats $\gamma = 1.4$.

There are two methods to extend the numerical schemes considered, namely by doing a componentwise extension and using characteristic decomposition. Liu and Osher [10] noted that high-order ENO/WENO schemes generate significant oscillations when solving hyperbolic systems unless costly characteristic decompositions are used. In the present work, we show that our new scheme is still efficient while adopting the less expensive componentwise extension for the stencil selection for each variable of U . The eigenvalues of the Jacobian matrix A are

$$\lambda_1(U) = q - a, \quad \lambda_2(U) = q, \quad \lambda_3(U) = q + a,$$

where $a = \sqrt{\gamma p / \rho}$ is the sound speed. We then use the Lax-Friedrichs flux for systems to find the values at the cell boundaries by the methods described previously

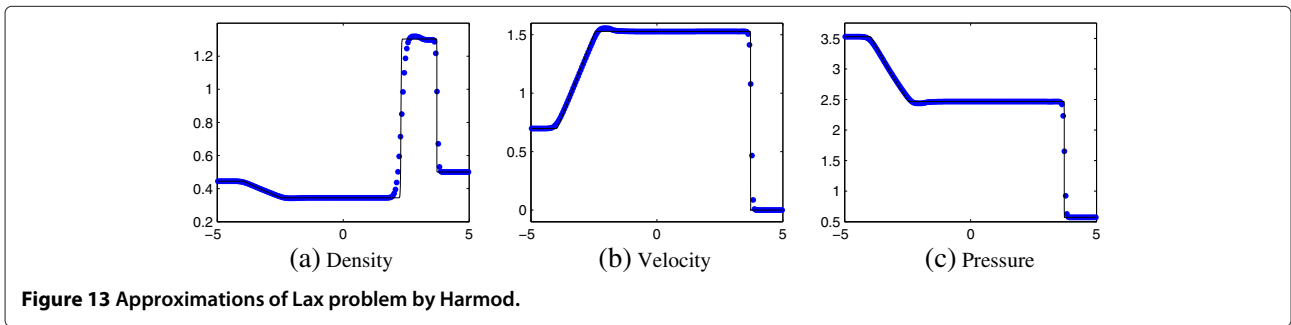
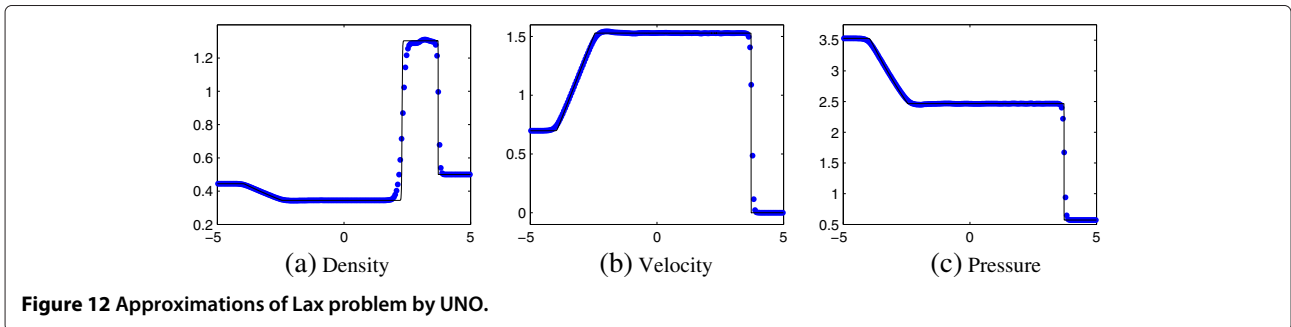


Table 3 CPU times of Sod and Lax shock tubes for $c=0.8$

Shock tubes	Number	MM1	MM2	UNO	Harmod	ENO2	ENO3
Sod	50	0.0318	0.0364	0.0390	0.0326	0.0269	0.0364
	100	0.0819	0.0932	0.1000	0.0829	0.0680	0.0940
	200	0.4310	0.4920	0.4990	0.4153	0.4679	0.5812
	400	1.2607	1.3641	1.6299	1.2589	1.1648	1.7618
Lax	50	0.0662	0.0763	0.0831	0.0685	0.0559	0.0793
	100	0.1763	0.2080	0.2258	0.1818	0.1483	0.2109
	200	0.7438	0.9097	1.2192	0.9168	0.7431	1.1855
	400	2.7978	3.1485	3.5679	2.9055	2.4790	3.8824

$$h(a, b) = \frac{1}{2} [f(a) + f(b) - \alpha(b - a)],$$

$$\alpha = \max_u \max_j |\lambda_j(u)|.$$

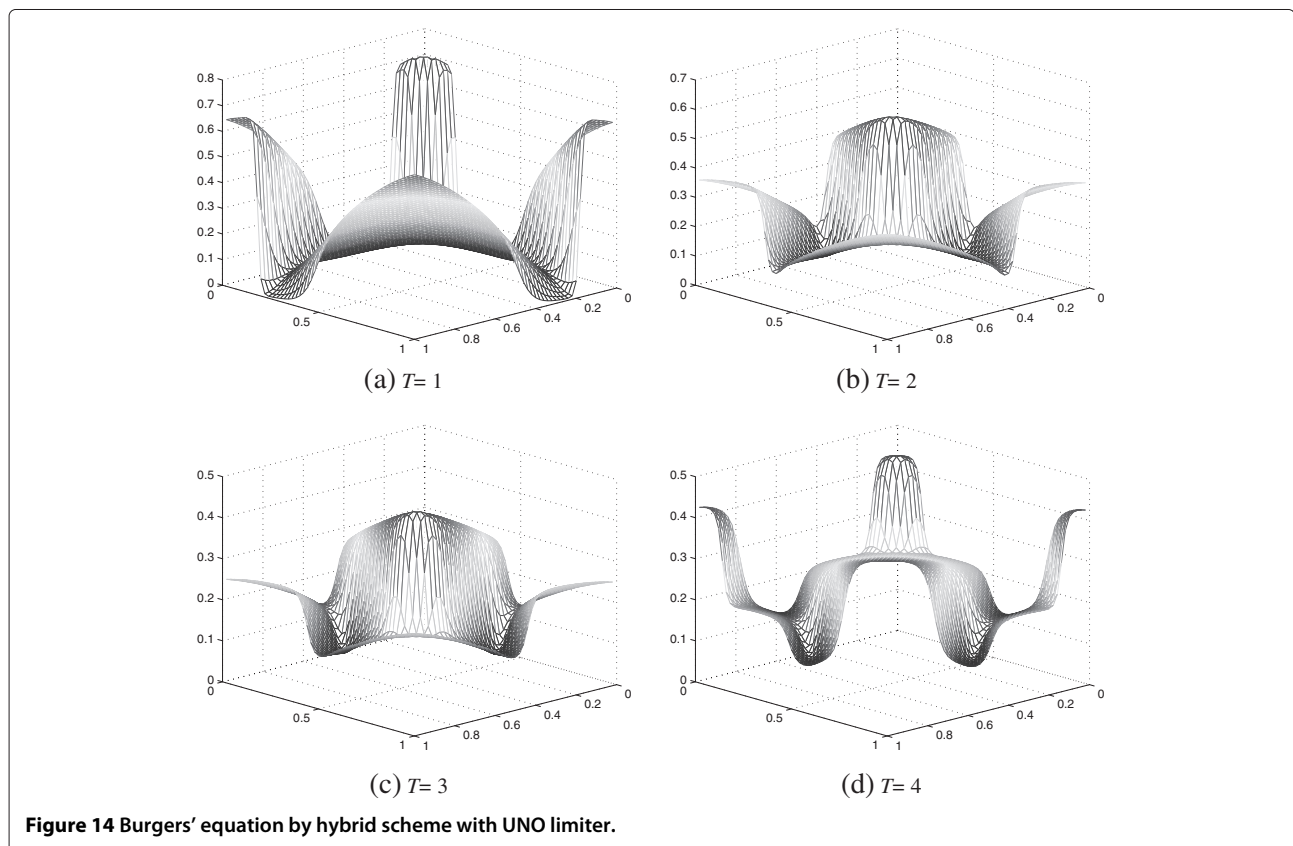
We test the numerical schemes for the Euler equations before the perturbations in the solutions reach the boundary of the computational domain on the interval $[-5, 5]$ with $c = 0.8$ using the third-order SSPRK scheme.

Sod problem

We solve the equations of gas dynamics (17) with the initial conditions given by [34]

$$U(x, 0) = \begin{cases} (1, 0, 2.5)^T, & -5 \leq x < 0, \\ (0.125, 0, 0.25)^T, & 0 \leq x \leq 5. \end{cases} \quad (18)$$

Figures 2, 3, 4, 5, 6 and 7 show the approximations obtained by the different schemes at time $T = 2$ for 200 cells. For this problem, ENO1 (not shown here) is too diffusive, while ENO3 has some oscillations successive to the expansion waves due to the lack of a mechanism to treat the oscillations still present near discontinuities. The scheme with the MM2 limiter presents overshooting because of the steep approximations of the slopes. Taylor series expansions carried out show that the hybrid



scheme with the MM1 limiter gives comparable results to ENO2, whereas the use of the other limiters present sharper approximations of the shocks.

Lax problem

Next, we solve (17) using the initial condition of [35]

$$U(x, 0) = \begin{cases} (0.445, 0.31061, 8.92840289)^T, & -5 \leq x < 0, \\ (0.5, 0, 1.4275)^T, & 0 \leq x \leq 5. \end{cases} \quad (19)$$

For this more severe shock tube problem, we show the different approximations on 200 cells at $T = 1.5$ in Figures 8, 9, 10, 11, 12 and 13. Similar to Sod's problem, the MM1 limiter with the hybrid scheme gives comparable results to ENO2. The hybrid scheme with the MM2 limiter produces some overshooting in the approximation of the density. For componentwise extension, the UNO and Harmod limiters give an overall good resolution with little smearing of the approximations of shocks for the velocity and pressure profiles, whereas ENO3 allows more oscillations in the numerical results of the velocity.

In Table 3, we give the CPU times for the different numerical solutions of the shock tube problems. We note that speed relationship of the schemes with componentwise extension is similar to scalar case.

Multi-dimension extension

In the 1D experiments, we demonstrated that the hybrid scheme with UNO limiter is similar to ENO3 on most problems for similar CPU times. Now, we extend the hybrid scheme with UNO limiter to solve 2D equations which can be generalized to multi-dimensional problems. Following the recommendations of [8], we use a finite difference approach for such problems. This technique is computationally less expensive than the finite volume technique for which quadrature rules are necessary. A more detailed explanation of finite difference schemes can be found in [3,8].

We solve Burgers' equation $u_t + (\frac{1}{2}u^2)_x + (\frac{1}{2}u^2)_y = 0$ for the initial condition from [36], $u(x, y, 0) = \sin^2(\pi x) \sin^2(\pi y)$, on the domain $[0, 1] \times [0, 1]$ with periodic boundary conditions. In Figure 14, we display the results up to $T = 4$ on 50×50 grid with $\lambda = 0.3$. We observe that the solutions are well resolved and non-oscillatory.

Conclusion

The implementation of ENO schemes requires many selection statements. In this paper, we have proposed ENO-flux limiter schemes which reduce the number of selection steps. These schemes are shown to use the large CFL numbers allowed by the SSPRK methods for the time evolution step. The new methods were based

on only one stencil selection, and we recovered third-order ENO reconstructions on smooth regions, which otherwise were only obtained after more selection steps. For some discontinuous problems, our numerical results indicated that the hybrid ENO-flux limiter schemes performed better and were computationally quicker to run as compared to some higher-order ENO schemes. When the limiter MM1 was used with the hybrid scheme, we got comparable results to ENO2. Applying the MM2 limiter produced sharper results on shocks, but it generated overshooting in the profiles of hyperbolic systems because of the steep approximations of the slopes. The hybrid schemes with UNO and Harmod limiters achieved the best resolved approximations, produced sharp resolutions of shocks and reduced the oscillations which may be present in ENO3. For hyperbolic systems, componentwise extensions were adopted instead of characteristic decompositions. We would like to mention that according to existing literature, for example [10], characteristic decompositions may reduce oscillations but at the expenses of more computations.

Competing interests

The authors declare that they have no competing interests.

Authors' contributions

AAIP contributed to the mathematical derivations and writing of the paper and carried out all numerical tests. DYT and MB contributed to the mathematical derivations and writing of the paper. All authors read and approved the final manuscript.

Acknowledgements

The authors thank the anonymous referees whose comments improved our work and the presentation of this paper. This work is dedicated with respect and appreciation to Professor Mahinder Kumar Jain.

Author details

¹Department of Applied Mathematical Sciences, University of Technology, Mauritius, La Tour Koenig, Pointe-aux-Sables, Mauritius. ²Department of Mathematics, University of Mauritius, Reduit, Mauritius.

Received: 30 April 2012 Accepted: 23 November 2012

Published: 23 March 2013

References

1. Harten, A, Engquist, B, Osher, S, Chakravarthy, S: Uniformly high order accurate essentially non-oscillatory schemes, III. *J. Comput. Phys.* **71**, 231–303 (1987)
2. Liu, XD, Osher, S, Chan, T: Weighted essentially non-oscillatory schemes. *J. Comput. Phys.* **115**, 200–212 (1994)
3. Jiang, GS, Shu, CW: Efficient implementation of weighted ENO schemes. *J. Comput. Phys.* **126**, 202–228 (1996)
4. Peer, AAI, Dauhoo, MZ, Bhuruth, M: A method for improving the performance of the WENO5 scheme near discontinuities. *Appl. Math. Lett.* **22**, 1730–1733 (2009)
5. Fjordholm, U, Mishra, S, Tadmor, E: Entropy stable ENO scheme. In *Proceedings of the 13th International Conference on Hyperbolic Problems: Theory, Numerics, Applications*, Beijing (2010)
6. Fjordholm, U, Mishra, S, Tadmor, E: ENO reconstruction and ENO interpolation are stable. *Found. Comput. Math.* **13**(2), 139–159 (2013)
7. Levy, D, Puppo, G, Russo, G: Central WENO schemes for hyperbolic systems of conservation laws. *Math. Model. Numer. Anal.* **33**(3), 547–571 (1999)
8. Shu, CW: Essentially non-oscillatory and weighted essentially non-oscillatory schemes for hyperbolic conservation laws. *Tech. Rep.*, 97–65, ICASE (1997)

9. Marquina, A: Local piecewise hyperbolic reconstruction of numerical fluxes for nonlinear scalar conservation laws. *SIAM J. Sci. Comput.* **15**(4), 892–915 (1994)
10. Liu, XD, Osher, S: Convex ENO high order multi-dimensional schemes without field by field decomposition or staggered grids. *J. Comput Phys.* **142**, 304–330 (1998)
11. Xu, Z, Shu, CW: Anti-diffusive flux corrections for high order finite difference WENO schemes. *J. Comput. Phys.* **205**, 458–485 (2005)
12. Rider, WJ, Greenough, JA, Kamm, JR: Combining high-order accuracy with non-oscillatory methods through monotonicity preservation. *Int. J. Numer. Meth. Fluids.* **47**, 1253–1259 (2005)
13. Rider, WJ, Greenough, JA, Kamm, JR: Accurate monotonicity- and extrema-preserving methods through adaptive nonlinear hybridizations. *J. Comput. Phys.* **225**, 1827–1848 (2007)
14. Costa, B, Don, WS: High order hybrid central-WENO finite difference scheme for conservation laws. *J. Comput. Appl. Math.* **204**, 209–218 (2007)
15. Serna, S, Marquina, A: Power ENO methods: a fifth-order accurate Weighted Power ENO method. *J. Comput. Phys.* **194**, 632–658 (2004)
16. Peer, AAI, Gopaul, A, Dauhoo, MZ, Bhuruth, M: New high-order ENO, reconstructions for hyperbolic conservation laws. In *Proceedings of the 2005 Conference on Computational and Mathematical Methods on Science and Engineering*, Alicante, Spain, 446–455 (2005)
17. Peer, AAI, Dauhoo, MZ, Gopaul, A, Bhuruth, M: A Weighted ENO-flux limiter scheme for hyperbolic conservation laws. *Int. J. Comput. Math.* **87**, 3467–3488 (2010)
18. Casper, J, Atkins, HL: A finite-volume high-order ENO scheme for two-dimensional hyperbolic systems. *J. Comput. Phys.* **106**, 62–76 (1993)
19. Casper, J, Shu, CW, Atkins, HL: Comparison of two formulations for high-order accurate essentially nonoscillatory schemes. *AIAA J.* **32**, 1970–1977 (1994)
20. Thornber, B, Mosedale, A, Drikakis, D: On the implicit large eddy simulations of homogeneous decaying turbulence. *J. Comput. Phys.* **226**, 1902–1929 (2007)
21. Zhang, R, Zhang, M, Shu, CW: On the order of accuracy and numerical performance of two classes of finite volume WENO schemes. *Commun. Comput. Phys.* **9**, 807–827 (2011)
22. van Leer, B: Towards the ultimate conservative difference scheme, V A second-order sequel to Godunov's method. *J. Comput. Phys.* **32**, 101–136 (1979)
23. Nessyahu, H, Tadmor, E: Non-oscillatory central differencing for hyperbolic conservation laws. *J. Comput. Phys.* **87**(2), 408–463 (1990)
24. Tadmor, E: Numerical viscosity and the entropy condition for conservative finite difference schemes. *Math. Comput.* **43**, 369–382 (1984)
25. Harten, A: High resolution schemes for hyperbolic conservation laws. *J. Comput. Phys.* **49**, 357–393 (1983)
26. Osher, S, Tadmor, E: On the convergence of difference approximations to scalar conservation laws. *Math. Comput.* **50**, 19–51 (1988)
27. Harten, A, Osher, S: Uniformly high-order accurate nonoscillatory schemes, I. *SIAM J. Numer. Anal.* **24**(2), 279–309 (1987)
28. Liu, XD, Osher, S: Nonoscillatory high order accurate self-similar maximum principle satisfying shock capturing schemes I. *SIAM J. Numer. Anal.* **33**(2), 760–779 (1996)
29. Liu, XD, Tadmor, E: Third order nonoscillatory central scheme for hyperbolic conservation laws. *Numer. Math.* **79**, 397–425 (1998)
30. Peer, AAI, Gopaul, A, Dauhoo, MZ, Bhuruth, M: A new fourth-order non-oscillatory central scheme for hyperbolic conservation laws. *Appl. Numer. Math.* **58**, 674–688 (2008)
31. Shu, CW, Osher, S: Efficient implementation of essentially non-oscillatory shock-capturing schemes. *J. Comput. Phys.* **77**, 439–471 (1988)
32. Shu, CW, Osher, S: Efficient implementation of essentially non-oscillatory shock-capturing schemes II. *J. Comput. Phys.* **83**, 32–78 (1989)
33. Gottlieb, S, Shu, CW, Tadmor, E: Strong stability-preserving high-order time discretization methods. *SIAM Rev.* **43**, 89–112 (2001)
34. Sod, G: A survey of several finite difference methods for systems of nonlinear hyperbolic conservation laws. *J. Comput. Phys.* **27**, 1–31 (1978)
35. Lax, PD: Weak solutions of nonlinear hyperbolic equations and their numerical computation. *Commun. Pure Appl. Math.* **7**, 159–193 (1954)
36. Levy, D, Puppo, G, Russo, G: A third order central WENO scheme for 2D conservation laws. *Appl. Numer. Math.* **33**, 415–421 (2000)

doi:10.1186/2251-7456-7-15

Cite this article as: Peer et al.: A hybrid ENO reconstruction with limiters for systems of hyperbolic conservation laws. *Mathematical Sciences* 2013 **7**:15.

Submit your manuscript to a SpringerOpen[®] journal and benefit from:

- Convenient online submission
- Rigorous peer review
- Immediate publication on acceptance
- Open access: articles freely available online
- High visibility within the field
- Retaining the copyright to your article

Submit your next manuscript at ► springeropen.com